Crystal size distribution analysis of quartz in sector- zoned of garnet schist using Back-scatter electron images

A. Rahimi-Chakdel[1], A. P. Boyle[2]

1- *Department of Geology, Faculty of Sciences, Golestan University, 49138-15739, Gorgan, Iran*
2- *Department of Earth Sciences, University of Liverpool, Liverpool, L69 3GP, U.K*

Abstract: The studied sample presents garnet textural sector-zoning as inclusions in two types in garnet schist from Morlaix, North-West Brittany, France. Crystal size distributions (CSD) of quartz crystals were measured in both types inclusions, in the matrix and strain shadows around garnet porphyroblasts using Back-scatter electron (BSE) images. The CSD plots of quartz crystals show an increase of average in sizes from type 1 inclusion,60μm, to the matrix,116 μm, and strain shadow,248 μm,. These differences could be explained of quartzes size distribution by many processes such as capturing by pophyroblast, crystal face, annealing and grain boundary migration

Introduction

Galwey and Jones [1] have suggested that measurement of size distribution of crystals may give evidence about the kinetics of the processes of nucleation and growth. However, Marsh [2], Cashman and Marsh [3], Cashman and Ferry [4], Johnes, Morgan & Galwey [5], Higgins [6-8] and Peterson [9] introduced interpretations of CSDs in igneous and metamorphic rocks which permit estimation of certain dynamic variables in magma and metamorphic rocks. Distinguishing populations of crystals with different size ranges can be an important step in understanding the dynamic history of a rock. In magmas, Paterson [9] has explained that crystal size distributions (CSDs) reflect crystal nucleation and growth rates, differential movement of melt and solids, and residence time in magma chambers. The crystal-size distributions (CSD) have been used to estimate the rate of crystal growth and identify the growth mechanism [8]. Higgins [8] presented a computer program that was used to calculate and plot CSDs. The program enables the conversion to be made simply. By using this program, crystal size distributions were investigated to obtain growth controls of quartz crystals which are in the matrix, strain shadows and pophyroblast on SEM backscatter electron (BSE) images in sector- zoned of garnet schist from Morlaix, France.

Geological setting

The area around Morlaix lies at a complex junction between three broad geological units. To the west, the León region is composed mainly of gneisses and schists intruded by Variscan granites (340-290 Ma). It has been proposed that Leon constitutes a separate geological affinity to southern Brittany. Further to the east of Morlaix, late Precambrain rocks and events predominate, with Brioverian metasediments and plutonic complexes deformed during the late Precambrain Cadonian orogeny. South of Morlaix, the North Armorican shear zone marks the northern boundary of the central Brittany region, within which both Brioverian and Lower Palaeozoic rocks show mainly the effects of Variscan deformation and metamorphism [10].The sample locality is at the south end of the Plage du Clouët, 2km south-east of Carentec and about 8 km north-west of Morlaix (Fig. 1). Power [10] has noted two main phases of deformation in

---

* Corresponding author, Tel: (0171) 4427173, Fax: (0171) 4427040, Email: rahimiaz@yahoo.co.uk

the Devonian and Carboniferous rocks from Morlaix. He implies that first phase (D$_1$) produced a strong foliation, generally parallel to bedding. A second phase (D$_2$) of deformation produced the obvious folding in the rocks. He suggests that the metamorphic grade of rocks around Morlaix is the lower greenschist facies of chlorite zone, characterised by the mineral assemblage quartz + muscovite + chlorite + albite. Chloritoid, garnet and staurolite are occurred with prograde metamorphism north-west of Morlaix. Garnets traced during the first deformation and are wrapped by the second deformation.

Method

Higgins [8] described how, ideally, crystal size distributions can be measured directly when crystals can be extracted quantitatively whole from a volume of rock, but accepts this is a rather unusual situation for most igneous rocks. He outlined that most CSD data are determined from two-dimensional sections through rock-outcrops, slabs, or thin sections. He also showed that these two-dimensional sections are images that need to be processed to extract various parameters describing the intersections, such as length, width, area, perimeter, orientation, and centroid location. Higgins [8] used stereological solutions to convert two-dimensional section data to three-dimensional CSDs. He divided these stereological solutions into direct and indirect methods. The direct method does not require assumptions about the particle shape and size distributions, whereas indirect methods do need such assumptions. He therefore divided the indirect method into parametric methods, where a size-distribution law is assumed, and distribution-free methods that are applicable to all distributions. The measured crystal length data of quartzes in Scion image were exported Higgins [8] CSD correction software length is defined here as being the greatest dimension of the intersection. All data were measured in millimetres and also crystal shapes were assumed to be blocks with dimensions 1:1:2.

The Ln (n) (n = number of crystals per unit volume, per unit length; units: mm^{-4}) against L (the crystal length, per mm) graphs (best fit graphs) were produced for each place (inclusions, the matrix and strain shadows) using Microsoft Office 2007. These show the population density (Ln (n$_0$)) and growth rate of the crystals and allowed the data to be seen in relation to the predicted linear trend. As presented above, population density is the total number of grains per unit volume, per unit length. This means that many grains in a small volume provide a high population density (e.g. quartz inclusions) whilst a few grains in a large volume give a small population density (e.g., strain-shadow quartzes). Growth is in terms of the actual time the crystal has spent growing. Thus, a crystal with a long growth time will be large (e.g., strain-shadow quartzes) and crystal with a short growth time will be small (e.g., quartz inclusions).
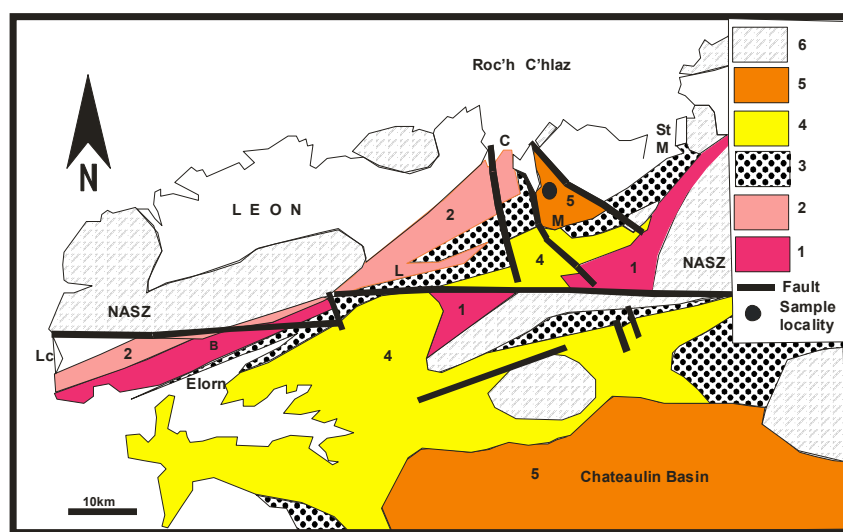

Figure. 1. Geological sketch map of north-west Brittany, France (after Power 1993) Place names: - B: Brest; C: Carantec; l: Landivisiau; Lc: Le Conquet; M: Morlaix; St M: St Michel-en-Greve; NASZ: north Armorican Shear Zone. Key: -1: Gneiss de Brest; 2: Le Conquest Schist; 3: Brioverian Supergroup; 4: Palaeozoic sedimentary rocks; 5: Carboniferous of Chateaulin and Morlaix; 6: Variscan granites.

Results
Sample description under Light microscopy
The studied sample (M1) was cut parallel to the stretching lineation and normal to the foliation. Sample M1 has an assemblage of garnet 24.8% + quartz 38.2% + muscovite 11% + chlorite 16.2% + rutile 0.6% + graphite 3.6% + opaque 5.6%. No biotite is present.

In thin section garnets have more or less regular textural sector-zoning (Figs. 2a, b and 3). The garnets are fresh sub-to euhedral in shape and 2 to 3 mm in diameter. The garnets are distributed in clusters throughout the rock without any obvious preferential distribution. Two foliations are present in the sample. The first foliation defined mainly by the shape orientation of muscovite and chlorite grains. The second foliation is wrapped around the garnet and areas where earlier fabrics may be preserved in the protected regions of lower strain either side of garnets.
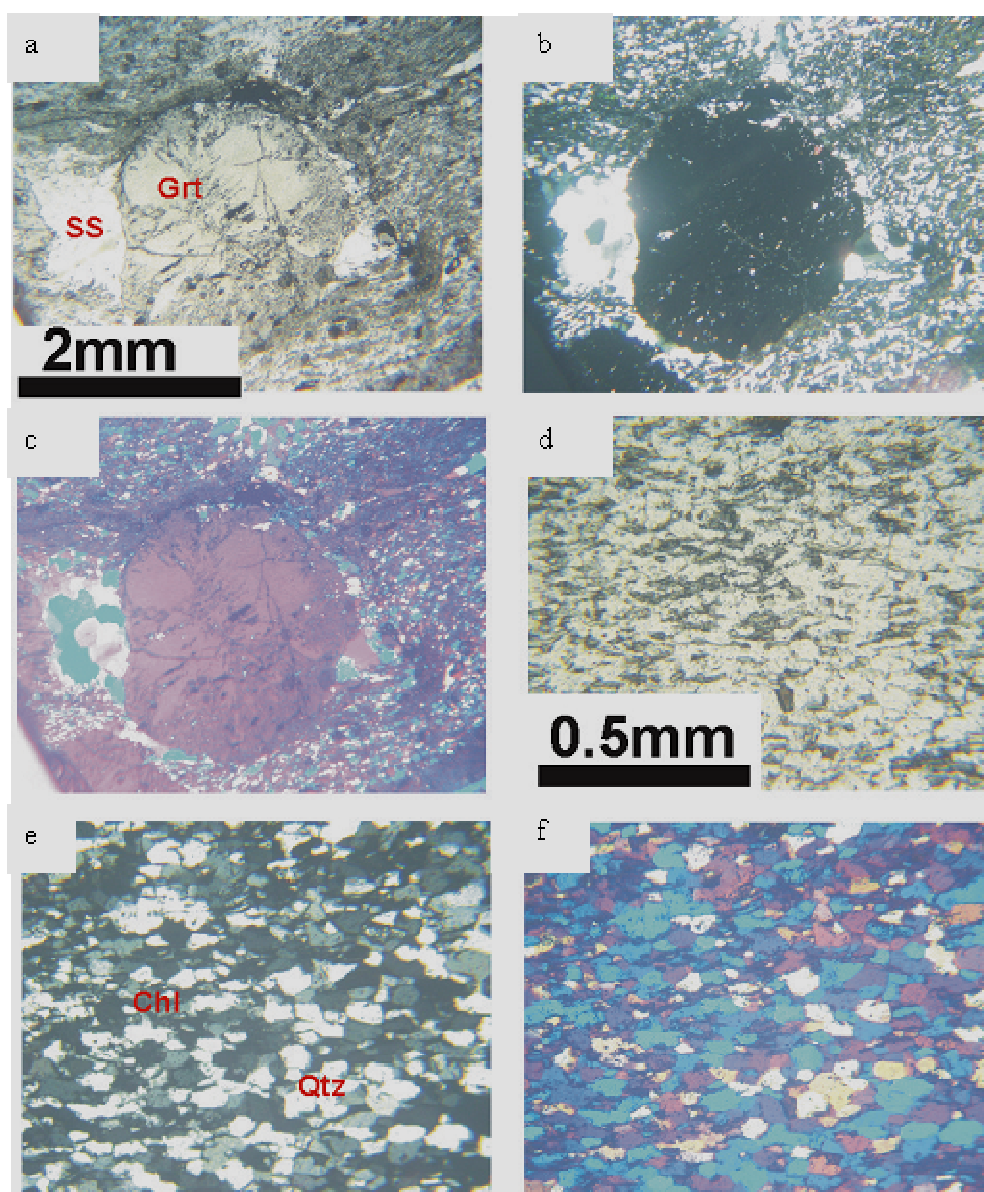

Figure. 2. Photomicrographs of garnet schist from Morlaix, North-West Brittany, France. (a) The wrapped garnet (Grt) porphyroblast with sector-zoning structure in PPL. (b) and (c) are the same area as (a) taken under XPL and XPL with gypsum plate, respectively. (d) The matrix shows elongation of quartz (Qtz), which is aligned under PPL. This alignment of quartz crystals defines lineation and foliation of sample. (e) and (f) the same area as (d) taken under XPL and XPL with gypsum plate respectively. SS = strain shadow, Chl = chlorite.
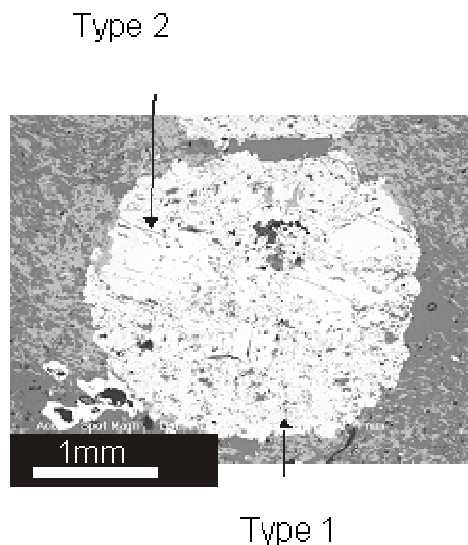
Type 2

Type 1

Figure 3. BSE image of poorly sector-zoned garnet shows rounded (Type1) and tubular (Type2) quartz inclusions garnet porphyroblast from sample M1.

All minerals in the matrix, except garnets, formed during the first phase of deformation [10]. Garnet growth overprinted the S_1 foliation demonstrating that garnet growth was after the formation of the S_1 foliation [12]. Later foliation (Figs. 2c and f) development (S_2) has wrapped the garnet porphyroblast during D_2-deformation [12]. Hence, it is suggested that garnets grew statically between the two deformations. Asymmetric strain shadows around garnet porphyroblasts were formed during D_2-deformation (Figs. 2a, b and c).The inclusions within the garnet are related to the sectorial growth of the garnets. However, most of the garnets have several rims of a different form of growth, with alternations of dusty graphite and quartz developed parallel to the crystal faces. It should be noted that electron microprobe analyses shows cores of garnets are manganese-rich, with the spessartine, almandine, grossularite and pyrope molecules present in approximately the proportions, 0.35: 0.45: 0.15: 0.05[10].

CSD analysis using BSE images from SEM
The sample M1 has been studied for geometrical aspect. This part was measured using BSE images. BSE images were used to determine CSD of quartz grains in garnets, the matrix and the strain shadows. Crystal size distributions were calculated using CSD Corrections 1.36 software [8, 11], which makes corrections for the intersection probability effect and partial corrections for the cut-section effect. The approximate particle shape and rock fabric were estimated by treating all quartz grains as ellipses in 2D sections. The long axis dimension of each grain was used in all CSD calculations.

CSD of quartz inclusions
CSD were measured for both types of quartz inclusions (Fig. 3). The Type 1 are more rounded with grain diameter ranges between 19-159 μm with an average size 60μm. Types 2 are more elongate with grain length ranges between 60-579μm with an average168μm. These data are plotted a CSD diagram in Fig. 6. Type 1 quartz inclusions show a steeper trend than the Type 2 inclusions.

CSD of the matrix quartz crystals
Two parts of the matrix were measured for CSD, totalling 158 quartz grains. The quartz crystals are separated from each other by phyllosilicates (Fig. 5). The quartz grains in the matrix show a range of grain diameters from 40 to 238 μm with an average grain size of 116 μm. These data are plotted as a CSD diagram (Fig. 6). The plot shows a more or less bell-shape size distribution of quartz crystals in the matrix.

CSD of quartz crystals in strain shadows
Asymmetric strain shadows are frequently described as the product of progressive deformation under a regime close to simple shear [13]. This feature allows the shear sense of the deformation to be determined. A clockwise rotation relative shear sense has been observed in sample M1 based on asymmetric strain shadows.

Strain shadows are filled essentially by quartz crystals (Fig.4d).

Quartz crystals in strain shadows have larger grain size than quartz in the matrix and inclusions. CSD measurements were made for 102 quartz crystals in strain shadows around two garnet porphyroblasts. Quartz crystals have grain diameter ranges between 64-541μm with an average grain size of 248 μm. Results are plotted in a CSD diagram (Fig. 6).
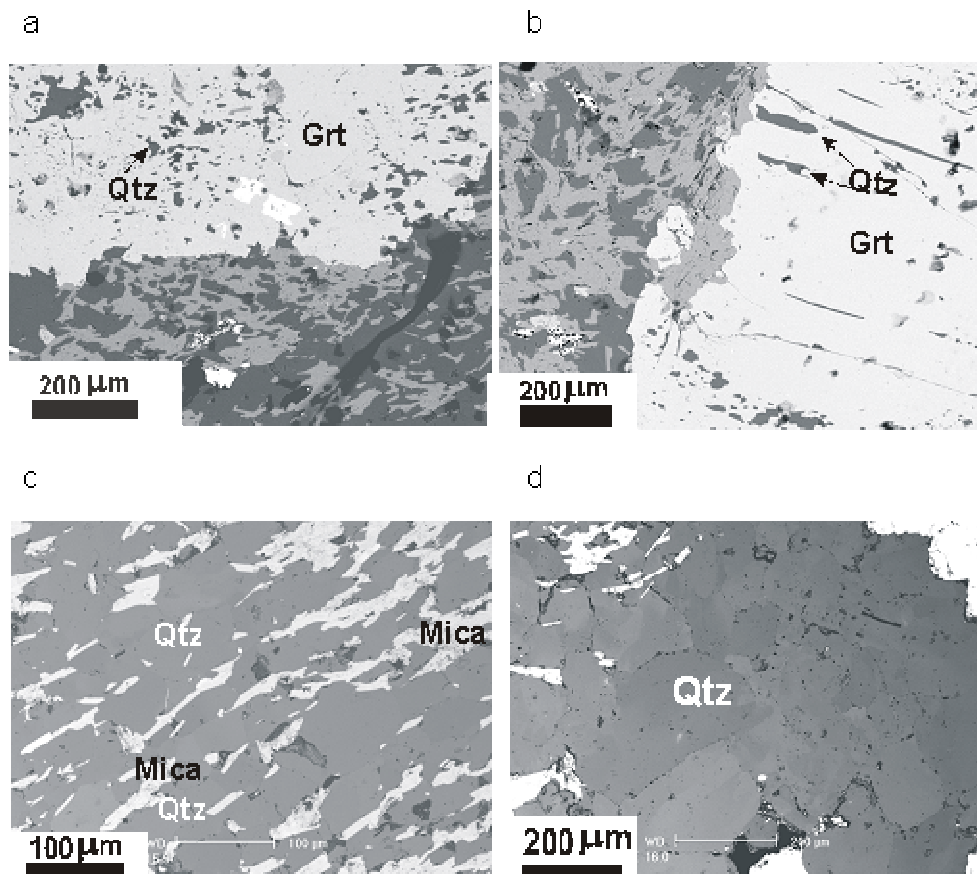

Figure 4. BSE images show the variety in size and shape of quartz (Qtz) crystals in the Type 1(a), Type 2 (b), the matrix (c) and strain shadows (d), respectively. Grt = garnet, Qtz = quartz
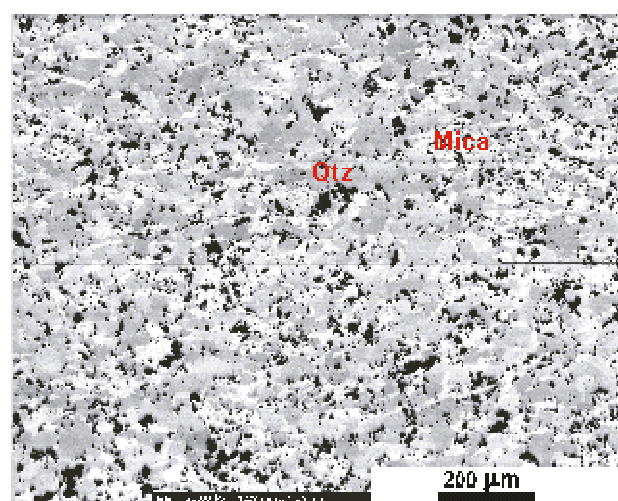

Figure 5. BSE image shows the matrix of sample M1 that has plenty of non-quartz minerals between to quartz crystals. Quartz shows up midgrey whereas phyllosilicates (mica) are light grey. The foliation is horizontal. Qtz = quartz
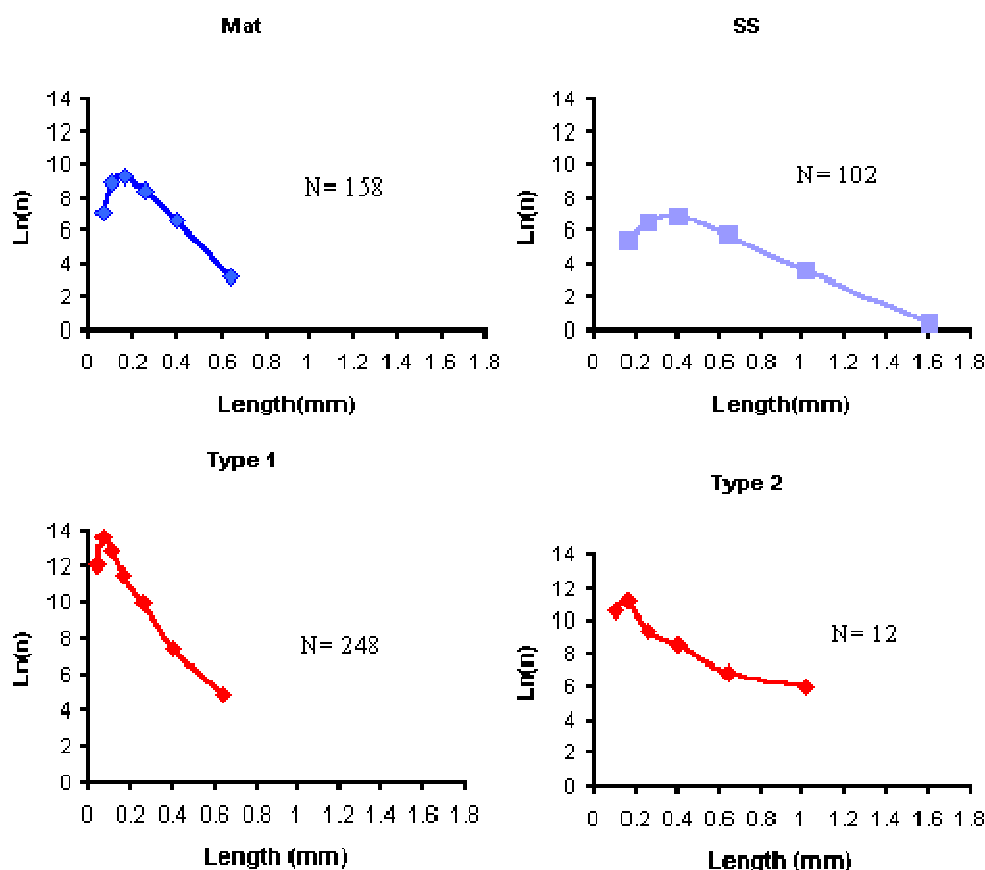
Figure 6. CSD plots for total quartzes in the matrix (Mat), strain shadow (SS) and both types of inclusions (Type 1, Type 2) from sample M1. N= number of crystals.

Comparison of CSD measurements in all parts

Numbers of quartz crystals per unit area as part of the comparison are summarised thus:

(1) 248 grains of inclusion Type 1 in an area 0.56 mm^2,

(2) 12 grains of inclusion Type 2 in an area 0.69mm^2,

(3) 158 grains of the matrix in an area 0.67 mm^2, and

(4) 102 grains of strain shadow in an area 0.57mm^2.

These CSD data show an increase in frequency of quartz crystals per unit area in the order from Type 2 inclusions, to strain shadows, to matrix to inclusion Type 1 inclusions (Fig. 7).

The following general points of CSD measurements can be summarized:

1- The CSD plots have shallower and negative at large crystal sizes of quartzes for all data sets (the matrix, strain shadow and porphyroblast inclusions).

2- The CSD plots at small crystal sizes have positive steep gradients of quartzes for all data sets (the matrix, strain shadow and porphyroblast inclusions).

3- The data for the smaller sizes are not linear whilst the larger sizes have approximately a straight line distribution for the quartz crystals in Type 1, the matrix and strain shadow (right hand limb of diagram).

4- The CSD plot of Type 1 quartz inclusion shows maximum number densities at the smallest size classes rather than in the intermediate grain sizes.

5- The CSD plot for quartz crystals in the matrix is more bell-shaped relative to other CSD plots of inclusions and strain shadow.

6- The matrix is relatively depleted in small quartz crystal sizes.

7- Strain-shadow quartz crystals tend to produce a shallower CSD slope than the matrix and inclusions.

The change in CSD characteristics of quartz crystals in order from inclusions, to matrix to strain shadow might be relate to garnet growth, increasing T, a decreasing strain rate. The total number of quartz crystals decreases with

increasing T in the matrix and decreasing strain in the strain shadows [14]. These changes involve an increase in average crystal size (Fig. 7). The change in number and average grain size of crystals would be expected from progressive degrees of annealing and decreases of strain rate because of the absent of other phases effect of annealing should be greater in strain shadows than in the matrix.

The right limbs of the matrix and strain shadow curves are linear, consistent with growth under conditions of temperature continuous [15]. Quartz inclusions formed at lower T than that finally experienced by the matrix quartz.

Discussion of quartzes CSD

The distribution of quartz grain sizes in sample M1 may be interpreted in terms of initial continuous nucleation and growth of quartz crystals, followed by a process such as Ostwald ripening (e.g. in the matrix). Thus, it would be expected that the quartz crystal size in all three parts of sample should be dependent on:

(i)   Annealing and dissolution;
(ii)   Capturing and protection by garnet porphyroblast;
(iii)   Grain boundary migration;
(iv)   Strain rate and magnitude.

Annealing and dissolution

The differences observed between quartz gains in garnet, the matrix and the strain shadow (summarised in Fig. 8) may be explained in terms of the differences in temperature and differential stress of the sample at the time these grains formed (or at least finished evolving). The CSD in the matrix is interpreted in terms of initial continuous nucleation and growth of crystals after the cessation of nucleation (Normal growth). The CSD diagram of the matrix and Type 1 quartzes shows a downturn at small grain sizes. They show a positive gradient at the smallest crystal sizes. A positive gradient must mean a negative growth rate [16].   In this case small crystals are being destroyed. Fig. 8 shows that the matrix-quartzes are relatively depleted in small crystals compared to inclusion quartzes (Type 1), but there are still a large number of relatively small grains, which shows the non-homogeneity of grain size in the matrix. The average size of the matrix-quartz is significantly coarser up to an order of magnitude than the typical inclusion (Type 1) size (Fig. 8), which suggests that a significant amount grain coarsening must have occurred in the matrix quartz after garnet growth. Depletion in the number of small quartz crystals in the matrix is probably due the process of annealing after garnet growth. The shape of CSD plot of the matrix (Fig.7) corresponds to Fig.1.8.d of [2], which suggests that the matrix quartz crystals grew under annealing process.
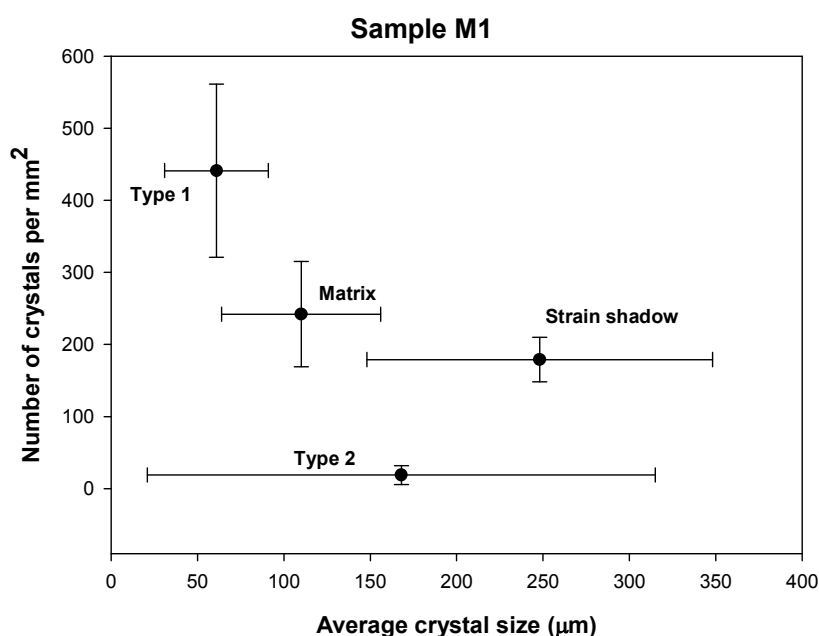

Figure 7. Quartz crystals are shown as number of crystals per mm^2 against average grain size in the matrix, strain shadows (SS), Type 1 and Type 2 inclusions from sample M1. Error bars indicate range of grain size (horizontal) and number of grains (vertical), respectively.
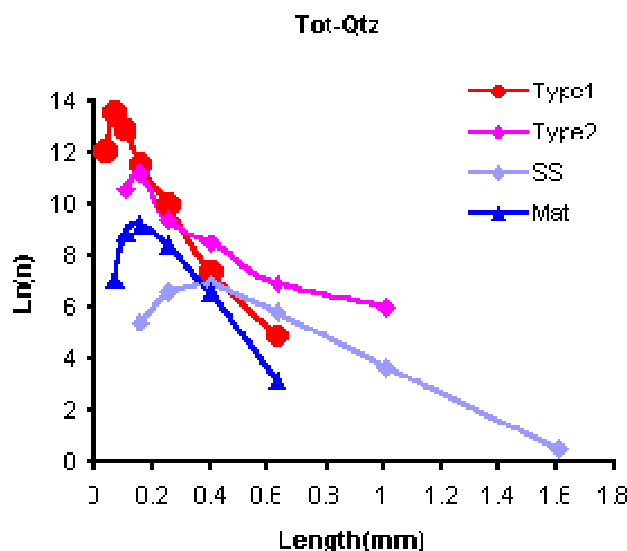
Figure 8. CSD plots of quartz crystals in sample M1. SS= total quartz crystals of both strain shadows, Inc= total quartz crystals of both inclusion types and mat= total quartz crystals in matrix

The average quartz grain size increases from inclusions to the matrix and strain shadows. This change in the size of quartz crystals may be explained by increased T. Quartz crystals in the matrix and strain shadows have been able to evolve over a longer period of elevated temperature, which may cause or enhance the annealing process. In this process grains will grow by grain boundary migration, which is aided by irregular shape and curved (Fig. 4d) quartz grain boundaries. These are more common in the strain shadows. In this model should be expected that larger quartz grains had grew by grain-boundary migration and smaller grains have decreased in size and ultimately they have been consumed in the matrix and strain shadow. Also, the effect of annealing should be greater in the strain shadow due to the lack of other minerals than in the matrix.

Capturing and protection by a garnet porphyroblast
CSD plots (Fig. 8) of Type 1 inclusions show the maximum number densities at the smallest size classes rather than in the intermediate grain sizes, which suggests that quartz inclusions (Type 1) had a relatively short growth period during early deformation periods and were then essentially preserved by garnet. In contrast, Type 2 inclusions show the maximum number of densities at the intermediate and largest value, which is consistent with simultaneous growth in garnet growth direction. Some Type 1 inclusions may have been partially dissolved during garnet growth. While classical CSD theory would suggest that Type 2 inclusions being longer, grew longer, it is perhaps more likely that they simply grew quicker or at least the same rate as the evolving garnet.

Grain boundary migration
The CSD of strain-shadow quartz plot shows shallower slope than the matrix and inclusions. This plot continues to larger sizes (Fig. 7). This may imply a higher growth rate for quartz crystals in the strain shadows. It is possible that strain shadow quartzes did not nucleate at the same time to the matrix and Type 1 quartz inclusions, but they have grown at a relatively rapid rate to relatively large grain sizes. The evidence suggests that quartz crystals coarsen in the strain shadows and recrystallized during deformation. There is an absence of non-quartz minerals between strain-shadow quartzes. This evidence can be explained

by the large dispersion in the size of quartz crystals in the strain shadows. Lack of non-quartz minerals (for example, mica and feldspar) between quartz grains in the strain shadows may be due to rapid growth [17]. This may leads grain boundary migration process in low strain zones of quartz coarsening.

Strain rate and magnitude

As mentioned before, quartz crystals in strain shadows grew in low strain zone relative to other parts in the matrix. Increased strain tends to result in smaller grain sizes [e.g. 18]. The low strain in strain shadow increased quartz growth rate respect to quartz crystals in the matrix. This observed difference is readily explained in terms of the differences in strain history, which may leads growth in quartz crystals in two areas (the matrix and the strain shadow).

Conclusion

The sample M1 exhibits two stage deformation histories. These two stages are responsible for the complex development of strain related structures crystal size distributions of quartz crystals in the matrix, strain shadows and both types inclusions in garnet. The CSD plots of quartz crystals show an increase of average in sizes from inclusion to the matrix and strain shadow. The small sizes of quartz crystals (Type 1) reflect record of initial matrix by porphyroblast whereas a larger size of Type 2 reflects intergrowth with crystal faces of host garnet. The size distribution of quartz crystals in the matrix reflects annealing process. The larger grain size in the strain shadows can be explained by grain boundary migration in domain lack of other minerals under low strain rate.

Acknowledgements

References

[1] Galwey A. K., Jones K. A., *"An attempt to determine the mechanism of a natural mineral-forming reaction from examination of the products"*, J chem. Soc London: (1963) 5681-5686

[2] Marsh B. D., *"Crystal size distribution (CSD) in rocks and the kinetics and dynamics of crystallization"*, Contributions to Mineralogy and Petrology, 99. (1988a) 277-291pp

[3] Cashman K. V., Marsh B. D., *"Crystal size distribution (CSD) in rocks and the kinetics and dynamics of crystallization"*, Contrib. Mineral. Petrol. Vol. 99 (1988) 292-305 pp.

[4] Cashman K. V., Frey J. M., *"Crystal size distribution (CSD) in rocks and the kinetics and dynamic of crystallization. Contrib"*, Mineral. Petrol. Vol. 99 (1988) 401-415 pp.

[5] Jones K. A., Morgan G.J., Galwey A. K., *"The significance of the size distribution function of crystals formed in metamorphic reactions"*, Chemical Geology, 9, (1972) 137-143 pp.

[6] Higgins M. D., *Numerical modelling of crystal shapes in thin sections: Estimation of crystal habit and true size.* American Mineralogist, Vol. 79, (1994) 113-119 pp.

[7] Higgins, M.D., *"Origin of anorthosite by textural coarsening: quantitative measurements of a natural sequence of textural development".* Journal of Petrology 39 (7), (1998)1307–1323.

[8] Higgins, M.D., *"Measurement of crystal size distributions".* American Mineralogist 85 (9), (2000)1105–1116.

[9] Peterson, T. D., *"A refined technique for measuring crystal size distributions in thin section".* Contrib. Mineral. Petrol. Vol. 124, (1996) 395-405 pp.

[10] Power, G. M. *"Groeth zoned manganese garnet in chloritoid, graphite schist near Morlaix, north-west France",* Annual conference of the Ussher Society 8, (1993) 132-137

[11] Higgins, M.D., *"Closure in crystal size distributions (CSD), verification of CSD calculations, and the significance of CSD fans".* American Mineralogist 87 (1), (2002) 171–175.

[12] Rahimi-Chakdel A., *"What controls the inclusion of quartz crystals in porphyroblasts: implications for texture analysis and tectonic*

interpretations"? Ph.D. Thesis, University of Liverpool, England (2003).

[13] Mainprice D. and Boudier F. A, *"Sense of shear in high temperature movement zones from fabric asymmetry of plagioclase feldspars"*. Journal of Structural Geology, 10, 1, (1988),73-81.

[14] Passchier C. W., Trouw R. A. J., *"Microtectonics"*, Springer - Verlog Berlin Heidelberg (1996).

[15] Randolph A. D., Larson M. A., *"Theory of particulate processes: Analysis and techniques of continuous crystallization",* Academic Press New York, (1971).

[16] Marsh B. D., *"Crystal size distribution (CSD) in rocks and the dynamics of crystallization",* Contrib. Mineral. Petrol. Vol. 99 (1988b) 277-291 pp.

[17] Ayers J. C., Miller C., Gorich B., Milleman J., *"Textural development of monazite during high-grade metamorphism: Hydrothermal growth kinetics, with implication for U, Th-Pb geochronology"*, American Mineralogist, Vol. 84, (1999)1766 -1780 pp.

[18] Kretz R., *"Grain-size distribution for certain metamorphic minerals in relation to nucleation and growth"*, The Journal of Geology, Vol. 74, No.2, (1966) 147-173 pp.